J Fluoresc (2014) 24:995–1001
DOI 10.1007/s10895-014-1408-x

RAPID COMMUNICATION

The Smart 2-(2-Fluorobenzoyl)-*N*-(2-Methoxyphenyl) Hydrazinecarbothioamide Functionalized as Ni(II) Sensor in Micromolar Concentration Level and its Application in Live Cell Imaging

Muhammad Saleem · Anser Ali · Chang-Shik Choi · Bong Joo Park · Eun Ha Choi · Ki Hwan Lee

Received: 16 March 2014 / Accepted: 19 May 2014 / Published online: 1 June 2014

Abstract In recent years, fluorescent probes for the detection of environmentally and biologically important metal cations have received extensive attention for designing and development of fluorescent chemosensors. Herein, we report the photophysical results of 2-(2-fluorobenzoyl)-*N*-(2-methoxyphenyl) hydrazinecarbothioamide (4) functionalized as Ni (II) sensor in micromolar concentration level. Through fluorescence titration at 488 nm, we were confirmed that ligand 4 showed the remarkable emission by complexation between 4 and Ni (II) while it appeared no emission in case of the competitive ions (Cr^{3+}, Fe^{2+}, Co^{2+}, Ba^{2+}, Cu^{2+}, Ca^{2+}, Na^{+}, K^{+}, Cu^{+}, Cs^{+}). Furthermore, ligand 4 exhibited no toxicity with precise cell permeability toward normal living cells using L929 cell lines in bio imaging experiment investigated through confocal fluorescence microscope. The non-toxic behavior of ligand 4 (assessed by MTT assay) and its ability to track the Ni^{2+} in living cells suggest its possibility to use in biological system as nickel sensor.

Keywords Fluorescent probe · Substituted thiosemicarbazide · Cytotoxicity · Cell permeability · Bioimaging

M. Saleem · K. H. Lee (✉)
Department of Chemistry, Kongju National University, Gongju, Chungnam 314-701, Republic of Korea
e-mail: khlee@kongju.ac.kr

A. Ali · B. J. Park · E. H. Choi
Department of Plasma Bioscience and display, Kwangwoon University, 20 Kwangwoon-gil, Nowon-gu, Seoul 139-701, Republic of Korea

C.-S. Choi
Department of Oriental Medicine Fermentation, Far East University, Eumseong Chungbuk 369-700, Republic of Korea

Introduction

The design and synthesis of fluorescent probes for sensing and monitoring of biologically and environmentally related transition metal ions is an attractive and fast growing field of research for chemistry, biology and environmental science due to their potential applications of high sensitivity and operational simplicity [1–4]. Accumulation of heavy metals like nickel in soils imposes great impact on soil fertility and hinders the effective supply of nutrients for vegetation [5–7]. Ni^{2+} introduced into the ecosystem through anthropogenic activities [8, 9] and industrial released results in metal settling in soil [10, 11] while water resources possessed the potential ability to transfer the metal ions in living organism [12–14]. Heavy metals can create adverse effects on the environment and human health due to their bioavailability and toxicity in various environmental components [15]. Human exposure to Ni^{2+} can cause number of disorders including skin irritation, lung fibrosis, cardiovascular diseases and cancer [16–18]. Therefore, first step toward nickel eradication from water and food material is the diagnosis of nickel by using simple analytical tools.

Herein, we report the synthesis of 2-(2-fluorobenzoyl)-*N*-(2-methoxyphenyl) hydrazinecarbothioamide (4) as fluorescent probe for the selective detection of Ni^{2+} in mixed aqueous-organic solution as well as explored the applicability of designed ligand for *in vitro* monitoring of nickel ions inside the living cells using L-929 cells (mouse fibroblast cells) under confocal fluorescence microscope. The results showed no toxicity and absolute cell permeability of synthesized ligand toward Ni^{2+} detection in mixed aqueous-organic solution and living cells with micro molar concentration level. The proposed nickel detection method possessed considerable advantages among several reported methods for nickel detection including potentiometric nickel sensation [19], high-

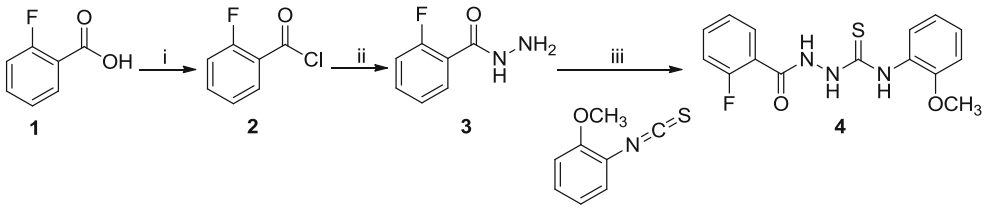

Scheme 1 Synthesis of 2-(2-fluorobenzoyl)-*N*-(2-methoxyphenyl) hydrazinecarbothioamide (4): Reagents and conditions: (i) $POCl_3$, $ClCH_2CH_2Cl$, reflux 3 h; (ii) hydrazine hydrate, TEA, MeCN, reflux 3 h; (iii) THF, stirring at ambient temperature, 18 h

resolution differential surface plasmon resonance sensor [20] and peptidase based nickel sensor [21] which involve complex detection methodology and complicated synthetic strategy.

Experimental

Substrate and Reagents

Substituted aromatic carboxylic acids and substituted aromatic isothiocyanate were purchased from Alfa Aesar. Hydrazine hydrate (80 %), sodium hydroxide and sodium bicarbonate were products of Aldrich. Ethanol, methanol, chloroform, water, DMF, MeCN, DCM (Samchun chemicals, Korea), H_2SO_4, HCl (Jin chemical & pharmaceutical Co. Ltd., Korea), $CrCl_3.6H_2O$, $FeCl_2.nH_2O$, $NiCl_2.6H_2O$, $CoCl_2.6H_2O$, $CuCl_2.2H_2O$, $BaCl_2.2H_2O$, $CaCl_2.2H_2O$, CsCl, CuCl, KCl, NaCl (Aldrich and Alfa Aesar) were used during experiment. The major chemicals utilized for biological studies includes MEM (minimum essential media, Wel Gene, Korea), FBS (fetal bovine serum, Bio west U.S.A.), Tripsin (Thermo scientific, South Loga, Utah), PBS (Wel Gene, Korea) and MTT [3-(4,5-dimethylthiazol-2-yl)-2,5-diphenyltetrazolium bromide, Sigma Aldrich, U.S.A.].

Instrumentations

Reaction progress was monitored by thin layer chromatographic (TLC) analysis and R_f values were determined by employing pre–coated silica gel aluminium plates, Kieselgel 60 F_{254} from Merck (Germany), using *n*–hexane : ethyl acetate, 8:2, as an eluent and TLC was visualized under UV lamp (VL–4. LC, France). Melting points were determined on Fisher scientific (USA) melting point apparatus and are uncorrected. Proton and carbon nuclear magnetic resonance (^1H and ^{13}C NMR) spectra were recorded on AVANCE 400, Frequency range: 400 MHz with TMS as an internal standard. Chemical shift are reported as δ values (ppm) downfield from internal tetramethylsilane of the indicated organic solution. Peak multiplicities are expressed as follows: s, singlet; bs, broad signal; m, multiplet and Ar-H, aromatic proton. Abbreviations are used as follows: DMSO-d_6, dimethyl sulfoxide-d_6; FT-IR spectroscopy, Fourier transform infrared spectroscopy. The fluorescence spectra and relative fluorescence intensities were measured on FS–2 fluorescence spectrometer (Scinco, Korea).

Synthesis of 2-(2-Fluorobenzoyl)-*N*-(2-Methoxyphenyl) Hydrazinecarbothioamide (4)

The substituted aromatic acid chloride 2 was synthesized by the reaction of substituted aromatic acid 1 (1 mmol) in the presence of 1, 2–dichloroethane (12 mL) as solvent and phosphorous oxychloride (0.4 mL) as chlorinating agent under reflux for 3 h, then the resulting solution was cooled to room temperature and solvent was removed under reduced pressure to afford substituted aromatic acid chloride 2 which was directly used for next step without further purification. The substituted aromatic acid chloride 2 was dissolved in acetonitrile (80 mL) and added drop wise into the solution containing hydrazine hydrate (1 mmol), triethyl amine (TEA, 0.5 mL), acetonitrile (20 mL) and allowed to reflux for 3 h, monitored by TLC. After consumption of the starting material, reaction mixture was cooled to room temperature. Evaporation of solvent under reduced pressure left crude aromatic acid hydrazide 3 as white solid on cooling, which was purified by column chromatography and crystallized on methanol [22]. The substituted aromatic acid hydrazides 3 (2 g, 1.17 mmol) were dissolved in THF (30 mL) and equimolar amount of substituted aromatic isothiocyanate (1.17 mmol) was separately dissolved in 20 mL of THF. Both of these solutions were mixed slowly and allowed to stir for 18 h, at room temperature, monitored by thin layer chromatography (TLC). On complete consumption of starting material, THF was

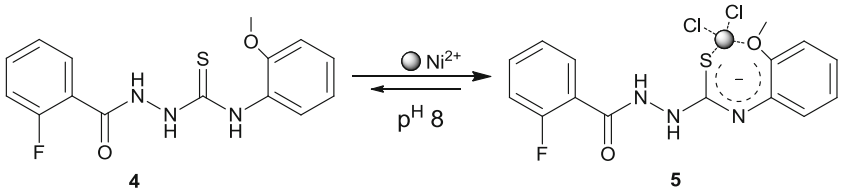

Scheme 2 The proposed chelation mechanism of ligand 4 upon $NiCl_2.6H_2O$ addition in acetonitrile/water (1:1, v/v) media

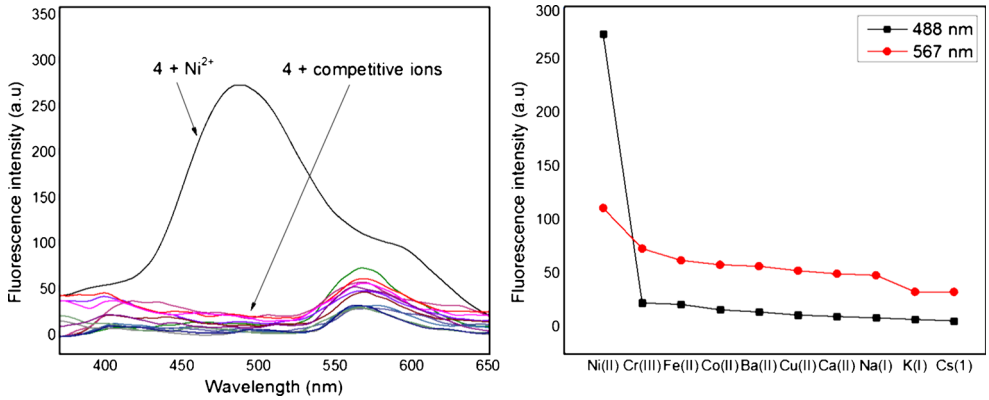

Fig. 1 Fluorescence emission spectra of ligand four (5 μM) in the presence of Ni^{2+} (5 μM) and competing ions (Cr^{3+}, Fe^{2+}, Co^{2+}, Ba^{2+}, Cu^{2+}, Ca^{2+}, Na^{+}, K^{+}, Cu^{+}, Cs^{+}) (5 μM) in aqueous/acetonitrile (1:1, v/v) solution, while excitation source was fixed to 388 nm during fluorescence emission spectral recording

evaporated on a rotary evaporator to leave behind corresponding hydrazinecarbothioamide 4 [23, 24] The synthesis of ligand 4 is schematically represented in Scheme 1.

2-(2-Fluorobenzoyl)-*N*-(2-Methoxyphenyl) Hydrazinecarbothioamide (4)

White solid; yield: 84 %; mp 131–133 °C; R_f: 0.31 (*n*–hexane : ethyl acetate, 8:2); FT-IR (ν/cm^{-1}): 3331, 3211 (NH), 1658, (C=O), 1551, 1536, 1498 (C=C), 1254 (C=S); ^{1}H NMR (400 MHz, DMSO-d_6) δ 9.95 (s, 1H, NH), 8.65 (bs, 1H, NH), 8.09 (bs, 1H, NH), 7.43–7.40 (s, 1H, Ar-H), 7.39–7.23 (m, 4H, Ar-H), 7.19–7.12 (m, 3H, Ar-H), 3.56 (s, 3H, OCH_3); ^{13}C NMR (100 MHz, DMSO-d_6) δ 178.6, 162.4, 159.3, 158.7, 135.6, 131.5, 130.5, 129.8, 125.4, 119.7, 118.2, 114.24, 114.1, 56.3; Anal. Calcd. for $C_{15}H_{14}FN_3O_2S$: C 56.41, H 4.42, N 13.16; Found: C 55.32, H 4.40, N 13.21 %.

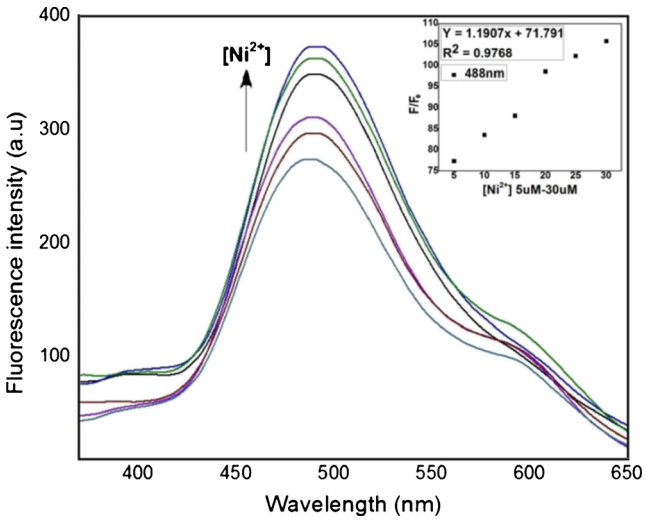

Fig. 2 The fluorescence titration of ligand 4 (5 μM) at emission maxima of 488 nm as a function of nickel ion concentration (5–30 μM, 1–6 equivalent), the inset described the fluorescence enhancement at emission maxima of 488 nm; F/F_O is determined as a ratio between the maximum fluorescence intensity (F, after Ni^{2+} addition) and minimum fluorescence intensity (F_O, free ligand 4 solution in absence of Ni^{2+}). Meanwhile, excitation source was fixed to 388 nm throughout fluorescence emission spectral recording

General Procedure for Spectroscopic Assay

A 500 μM stock solution of ligand 4 was prepared by dissolving 1.59 mg ligand 4 in methanol (total volume 10 mL). Similarly, to prepare 500 μM nickel stock solution, 1.18 mg of nickel (II) chloride hexahydrate was dissolved in distilled water (total volume 10 mL). All the metal ions solutions were prepared similar as Ni^{2+} stock solution. For spectroscopic measurements, test solution of 1 mL was prepared with 880 μL of 50 % aqueous acetonitrile, 10 μL of ligand stock solution, 100 μL of buffer solution (10 mM) and 10 μL of Ni^{2+} stock solution. The resulting solution were mixed before measurement and final volume was fixed as 1 mL for UV-visible and fluorescent measurement using [SCINCO] UV–vis Spectrophotometer "S-3100" and FS–2 fluorescence spectrometer (SCINCO, Korea), respectively.

General Procedure for MTT Assay

MTT assay was done following the reported procedure [25]. Briefly, the cells were incubated with Ni^{2+} (50 μM) and ligand

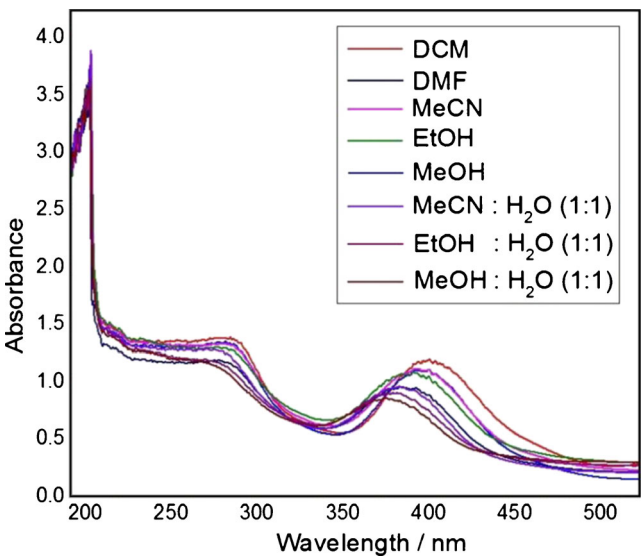

Fig. 3 Effect of various solvent on the UV-visible absorption spectrum of ligand 4 (5 μM) in the presence of nickel ion (5 μM)

Table 1 The optical characteristics of 4 in the presence of Ni^{2+} in various solvents

Solvents	$\pi \rightarrow \pi^*$		$n \rightarrow \pi^*$	
	λ_{max} (nm)	Molar absorptivity (M^{-1} cm^{-1})	λ_{max} (nm)	Molar absorptivity (M^{-1} cm^{-1})
DCM	294	2.74×10^5	402	2.40×10^5
DMF	294	2.72×10^5	400	2.22×10^5
MeCN	294	2.68×10^5	400	2.18×10^5
MeOH	294	2.60×10^5	396	2.16×10^5
EtOH	288	2.52×10^5	392	1.90×10^5
MeCN:H_2O (1:1)	290	2.38×10^5	388	1.90×10^5
MeOH:H_2O (1:1)	288	2.34×10^5	388	1.80×10^5
EtOH:H_2O (1:1)	288	2.32×10^5	388	1.72×10^5

4 (60 μM) for 24 hours. Then cells were washed with phosphate buffered saline (PBS), and incubated with Dulbecco's Modified Eagle's medium (DMEM medium, 200 μL/well) containing 50 μL of MTT [3-(4,5-dimethylthiazol-2-yl)-2, 5-diphenyltetrazolium bromide, 5 mg/mL] solution. Following 2 hours incubation at 37 °C, growth medium was removed gently from the plate and 200 μL/well dimethyl sulfoxide was added to solubilize the produced purple formazan crystals. Later, the absorbance for each well was measured at 570 nm using microplate spectrophotometer systems (BioTek, synergy HT) and results were calculated in percentage with respect to untreated sample called control.

Results and Discussions

The spectroscopic properties of compound 4 (5 μM) were measured in aqueous/acetonitrile (1:1, v/v) solution before and after addition of Ni^{2+} (5 μM). The compound 4 did not show any significant fluorescent signal at 488 nm under 388 nm excitation in the fluorescence emission spectrum as well as at 388 nm in the fluorescence excitation spectrum when 488 nm emission was fixed in the absence of nickel ion, while it was detected a prominent signal with emission maxima of 488 nm and excitation maxima of 388 nm after nickel addition. The proposed mechanism for this fluorescence appearance in the compound 4 solution upon Ni^{2+} addition are shown in Scheme 2.

It was supposed that the reason for fluorescence signal enhancement was due to the partial generation of quinoline like structure in 4 after ligand-nickel chelation. The Ni^{2+} triggered newly adopted conformational structure of compound 4 into 5 exhibited more delocalization of electronic cloud which ultimately decreased the band gap energy between HOMO and LUMO and caused the rapid electronic transition in the visible range of spectrum, while other common ions (Cr^{3+}, Fe^{2+}, Co^{2+}, Ba^{2+}, Cu^{2+}, Ca^{2+}, Na^+, K^+, Cu^+, Cs^+) did not show any emission signal at 488 nm after addition to ligand 4 solution. However, there was a slight signal appearance at longer wavelength for ligand solution in the presence of almost all metal ions at 567 nm with no selectivity for any metal ions as shown in Fig. 1.

To gain more insight into the behavior of 4 towards Ni^{2+}, the fluorescence titration experiment was conducted which revealed that the fluorescence intensity of ligand solution gradually increased with increasing concentration of nickel ions in aqueous/acetonitrile (1:1, v/v) media as shown in Fig. 2. From this titration experiment, the minimum detection ability of ligand 4 for Ni^{2+} was expected to be 5 μM from the inset of Fig. 2 and the value of linearly dependent co-efficient (R^2) was found to be 0.9768 (inset of Fig. 2).

The absorption of ligand-Ni^{2+} complex was recorded in different solvents of varying types (Fig. 3). The main absorption band of ligand-Ni^{2+} complex showed solvent dependence with a negative solvatochromism, *i.e.*, blue shift with increasing solvent polarity as shown in Table 1. This absorption band change suggest that in the ground state the ligand-Ni^{2+}

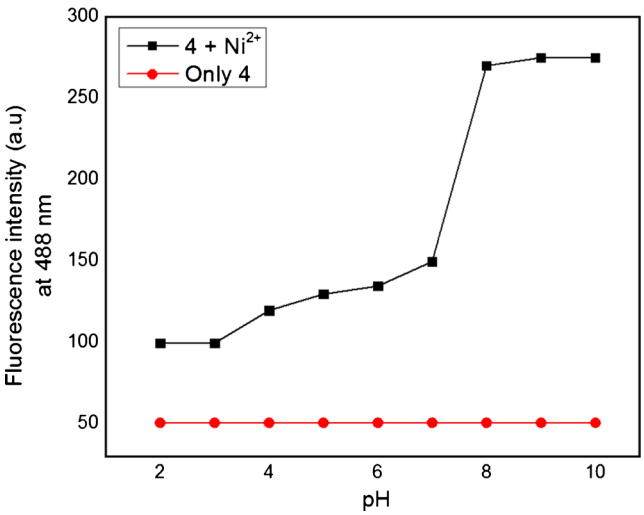

Fig. 4 Fluorescence intensity variation at maximum emission of 488 nm, with alteration of pH from 2 to 10, in the buffer solution

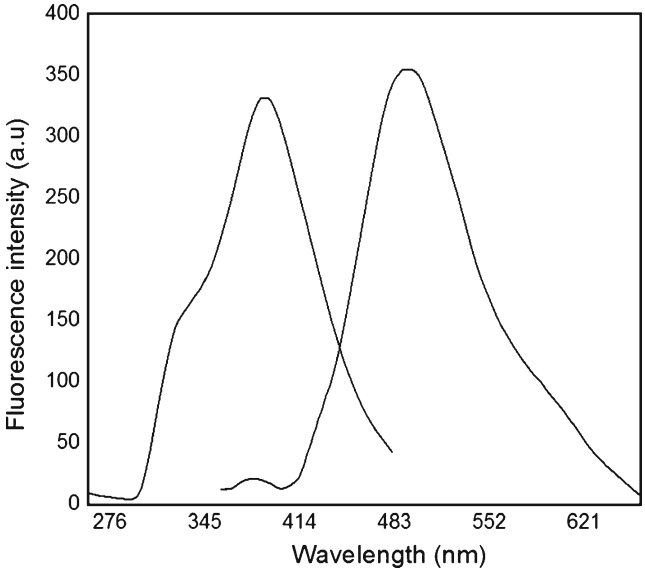

Fig. 5 Fluorescence excitation and emission spectrum of 4 in the presence of Ni^{2+} in aqueous/acetonitrile (1:1, v/v) media

complex interacts more with a protic solvent, while the excited state is preferentially stabilized in the presence of an aprotic solvent. For fluorescence emission spectral recording, the excitation wavelength was fixed at 388 nm, Ex. Slit=5 nm, Em. Slit=5 nm, Ex. Filter = air, Em. Filter = air, repeat number=1, repeat interval time (m)=1, PMT voltage (v)= 700, Scan speed (nm/min)=60, Integration time (ms)=5 and Response time (s)=0.02.

The effects of various solvents on the optical properties of ligand-Ni^{2+} complex along with their extinction coefficient or molar absorptivity (ε) [26, 27] values are tabulated in Table 1.

The effect of pH was evaluated in the pH range of 2–10 in the buffer solution. The maximum emission intensity was observed in the basic pH condition while there was low intensity signal in the acidic pH. These results indicate that Ni^{2+} showed complexation with maximum tendency in the deprotonated conformation of ligand 4 as depicted in the Scheme 2, while ligand 4 alone do not show any emission signal in the pH span of 2–10 as shown in Fig. 4.

The ligand 4 exhibited significant Stokes shift of 5,283 cm^{-1} for easy separation of excitation and emission signal as shown in Fig. 5, calculated by the reported methods [28]. The larger Stokes shift and longer wavelength chromophore considered to be more compatible for sensing and intracellular cell imaging [29–32].

The fluorescent quantum yield of compound 4 was almost zero before nickel addition to its reaction solution, while after nickel introduction into probe solution, the relative fluorescence quantum yield of 0.032 was observed by employing quinine sulfate (0. 05 M stock solution in 0.1 N sulfuric acid) as standard for relative fluorescence quantum yield measurement [33–36].

Bioimaging Applications of Ligand 4 in L-929 Cell Lines

To investigate the capability of the ligand four toward Ni^{2+} in biological samples, fluorescence imaging experiments were performed. In this imaging study L-929 cells, established from the normal subcutaneous adipose and areolar tissue of a male mouse were used following the reported procedure [37] with some modifications. Briefly, cells were incubated with ligand 4 (60 μM) in complete DMEM (Dulbecco's Modified Eagle medium) for 6 hours at 37 °C, and very weak fluorescence was observed. After washing with PBS twice, the samples were treated with Ni^{2+} (0 and 50 μM) and incubated for more 6 hours at 37 °C, which displayed distinct intracellular fluorescence at 50 μM nickel ions concentration as shown in Fig. 6.

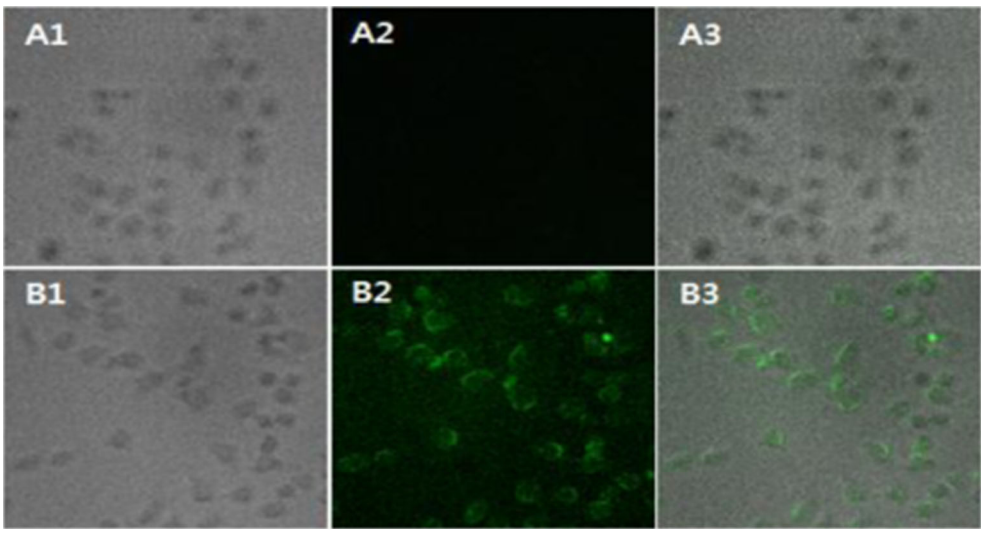

Fig. 6 Confocal fluorescence microscopic images for intracellular Ni^{2+} detection with ligand 4 employing L-929 cells; (A1-A3) cells incubated with probe (60 μM); (B1-B3) cells incubated with probe (60 μM) in the presence of nickel ion (50 μM). While A1, B1: bright field images; A2, B2: fluorescence images and A3, B3: merged images

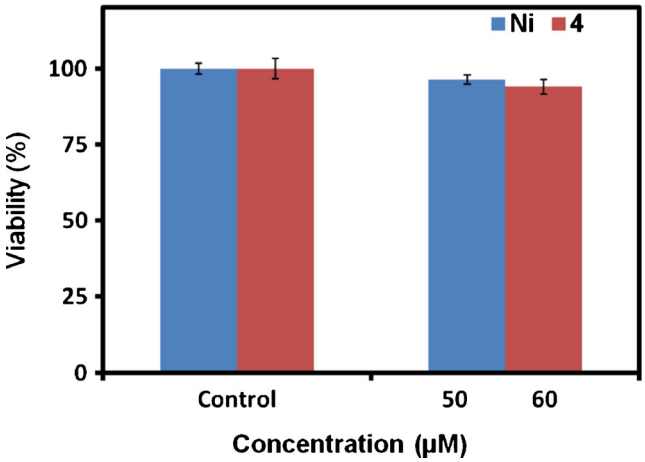

Fig. 7 Viability of L-929 cells cultured in complete DMEM with 60 μM of ligand 4 and 50 μM of nickel ions, respectively while the control cells were cultured in the medium without ligand and nickel ions

Cytotoxicity Assay

The ligand safety was assessed after 24 hours treatment to the cells by MTT [3-(4, 5-dimethylthiazol-2-yl)-2, 5-diphenyltetrazolium bromide] assay. The results showed no toxicity for L-929 cells at 60 μM ligand and 50 μM nickel ions concentrations as showed in Fig. 7. The non-toxic behavior of ligand 4 and its ability to track the Ni^{2+} in living cells suggest its possibility to use in biological system as nickel sensor.

Conclusion

In summary, 2-(2-fluorobenzoyl)-*N*-(2-methoxyphenyl) hydrazinecarbothioamide (4) has been introduced as nickel ion sensor in mixed aqueous-organic media. The photophysical properties of synthesized ligand 4 exhibited the fluorescence emission signal at 488 nm and fluorescence excitation signal at 388 nm upon nickel ligation which was considered due to partial generation of quinoline like structure in four by ligand-nickel chelation. Furthermore, for practical applicability, bio imaging experiment was conducted using L-929 cell lines. The ligand four showed no toxicity with absolute cell permeability for the tested cell lines. These results depicts that the newly synthesized ligand 4 can be used as selective nickel sensing platform in mixed aqueous-organic solution and inside living cells with considerable fluorescence response in the visible region.

Acknowledgments This research was supported by the Basic Science Research Program through the National Research Foundation of Korea (NRF) funded by the Ministry of Education, (No. 2011–0015056) and the National Research Foundation of Korea (NRF) grant funded by the Korea government (MSIP) (NRF-2010-0027963).

References

1. Wang H, Wang D, Wang Q, Li X, Schalley CA (2010) Nickel (II) and iron (III) selective off-on-type fluorescence probes based on perylene tetracarboxylic diimide. Org Biomol Chem 8:1017–1026
2. Moro AV, Ferreira PC, Migowski P, Rodembusch FS, Dupont J, Ludtke DS (2013) Synthesis and photophysical properties of fluorescent 2,1,3-benzothiadiazole-triazole-linked glycoconjugates: selective chemosensors for Ni (II). Tetrahedron 69:201–206
3. Abebe FA, Eribal CS, Ramakrishna G, Sinn E (2011) A 'turn-on' fluorescent sensor for the selective detection of cobalt and nickel ions in aqueous media. Tetrahedron Lett 52:5554–5558
4. Goswami S, Chakraborty S, Paul S, Halder S, Maity AC (2013) A simple quinoxaline-based highly sensitive colorimetric and ratiometric sensor, selective for nickel and effective in very high dilution. Tetrahedron Lett 54:5075–5077
5. Qu M, Li W, Zhang C (2013) Assessing the risk costs in delineating soil nickel contamination using sequential Gaussian simulation and transfer functions. Ecol Inform 13:99–105
6. Quantin C, Ettler V, Garnier J, Sebek O (2008) Sources and extractibility of chromium and nickel in soil profiles developed on Czech serpentinites. Geoscience 340:872–882
7. Radziemska M, Mazur Z, Jeznach J (2013) Influence of applying halloysite and zeolite to soil contaminated with nickel on the content of selected elements in maize (Zea mays L.). Chem Eng Trans 32: 301–306
8. Ruan YB, Yu Y, Li C, Bogliotti N, Tang J, Xie J (2013) Triazolyl benzothiadiazole fluorescent chemosensors: a systematic investigation of 1,4- or 1,5-disubstituted mono- and bis-triazole derivatives. Tetrahedron 69:4603–4608
9. Vandenbrouck T, Dom N, Novais S, Soetaert A, Ferreira ALG, Loureiro S, Soares AMVM, Coen WD (2011) Nickel response in function of temperature differences: Effects at different levels of biological organization in Daphnia magna. Comp Biochem Physiol 6:271–281
10. Patel E, Lynch C, Ruff V, Reynolds M (2012) Co-exposure to nickel and cobalt chloride enhances cytotoxicity and oxidative stress in human lung epithelial cells. Toxicol Appl Pharmacol 258:367–375
11. Yeganeh M, Afyuni M, Khoshgoftarmanesh AH, Khodakarami L, Amini M, Soffyanian AR, Schulin R (2013) Mapping of human health risks arising from soil nickel and mercury contamination. J Hazard Mater 244–245:225–239
12. Xiel J, Funakoshi T, Shimada H, Kojima S (1995) Effects of chelating agents on testicular toxicity exposure to nickel. Toxicology 103: 147–l 55
13. Novelli ELB, Hernandes RT, Filho JLVBN, Barbosa LL (1998) Differential/combined effect of water contamination with cadmium and nickel on tissues of rats. Environ Pollut 103:295–300
14. Rathor G, Adhikari T, Chopra N (2013) Management of nickel contaminated soil and water through the use of carbon nano particles. J Chem Bio Phy Sci Sec A 3:901–905
15. Sharma V, Sachdeva MV, Sakhuja N, Arora D (2011) Impact of heavy metals (Chromium and Nickel) on the health of residents of Jagadhri city due to intake of contaminated underground water. Arch Appl Sci Res 3:207–212
16. Denkhaus E, Salnikow K (2002) Nickel essentiality, toxicity, and carcinogenicity. Crit Rev Oncol Hematol 42:35–56
17. Kasprzak KS, Sunderman FW, Salnikow K (2003) Nickel carcinogenesis. Mutat Res 533:67–97
18. Dodani SC, He Q, Chang CJ (2009) A turn-on fluorescent sensor for detecting nickel in living cells. J Am Chem Soc 131:18020–18021
19. Kumar P (2012) All solid state nickel (II)-selective potentiometric sensor based on an upper Rim substituted calixarene. Electroanalysis 24:2005–2012

20. Forzani E, Zhang H, Chen W, Tao N (2005) Detection of heavy metal ions in drinking water using a high-resolution differential surface plasmon resonance sensor. Environ Sci Technol 39:1257–1262
21. Lv XL, Luo SZ (2012) A fluorescence chemosensor based on peptidase for detecting nickel (II) with high selectivity and high sensitivity. Anal Bioanal Chem 402:2999–3002
22. Huang J, Xu Y, Qian X (2009) A Rhodamine-based Hg^{2+} sensor with high selectivity and sensitivity in aqueous solution: a NS2-containing receptor. J Org Chem 74:2167–2170
23. Yang YK, Yook KJ, Tae J (2005) A rhodamine-based fluorescent and colorimetric chemodosimeter for the rapid detection of Hg^{2+} ions in aqueous media. J Am Chem Soc 127:16760–16761
24. Dolman SJ, Gosselin F, Shea PDO, Davies IW (2006) Superior reactivity of thiosemicarbazides in the synthesis of 2-amino-1,3,4-oxadiazoles. J Org Chem 71:9548–9551
25. Mosmann T (1983) Rapid colorimetric assay for cellular growth and survival: application to proliferation and cytotoxicity assays. J Immunol Methods 65:55–63
26. Edelhoch H (1967) Spectroscopic determination of tryptophan and tyrosine in proteins. Biochemistry 6:1948–1954
27. Gill SC, Hippel PH (1989) Calculation of protein extinction coefficients from amino acid sequence data. Anal Biochem 182:319–326
28. Georgiev NI, Sakr AR, Bojinov VB (2011) Design and synthesis of novel fluorescence sensing perylene diimides based on photoinduced electron transfer. Dyes Pigm 91:332–339
29. Lang K, Chin JW (2013) Fluorescent imaging: shining a light into live cells. Nat Chem 5:81–82
30. Lin W, Buccella D, Lippard SJ (2013) Visualization of peroxynitrite-induced changes of labile Zn^{2+} in the endoplasmic reticulum with benzoresorufin-based fluorescent probes. J Am Chem Soc 135: 13512–13520
31. Guo T, Cui L, Shen J, Wang R, Zhu W, Xu Y, Qian X (2013) A dual-emission and large stokes shift fluorescence probe for real-time discrimination of ROS/RNS and imaging in live cells. Chem Commun 49:1862–1864
32. Xue L, Liu C, Jiang H (2009) A ratiometric fluorescent sensor with a large Stokes shift for imaging zinc ions in living cells. Chem. Commun. 1061–1063.
33. Demas JN, Crosby GA (1971) The measurement of photoluminescence quantum yields. A Review J Phys Chem 75: 991–1024
34. Wurth C, Grabolle M, Pauli J, Spieles M, Genger UR (2013) Relative and absolute determination of fluorescence quantum yields of transparent samples. Nat Protoc 8:1535–1550
35. Lakowicz JR (2006) Principles of fluorescence spectroscopy, 3rd edn. Springer science + business media, LLC, New York, pp 54–55
36. Brouwer AM (2011) Standards for photoluminescence quantum yield measurements in solution (IUPAC Technical Report). Pure Appl Chem 83:2213–2228
37. Fanyong Y, Donglei C, Ning Y, Meng W, Linfeng D, Chuying L, Li C (2013) A rhodamine based fluorescent probe for Hg^{2+} and its application to cellular imaging. Spectrochim. Acta, Part A 106:19–24